Periodicals of Engineering and Natural Sciences ISSN 2303-4521
Vol. 8 , No. 3, July 2020, pp.1345-1358

Design and evaluation of optical laser diodes LD positioning arrangement and multiple input/ multiple output MIMO-OFDM systems

Faris Mohammed Ali [1], Bashar J. Hamza[2], Yassen H. Taher[3]

[1,2]Department of Communications Techniques Engineering, Engineering Technical College, Al-Furat Al-Awsat Technical University, Al-Najaf 31001, Iraq.

[3]Department of Power Electric Engineering, Technical Engineering College\Basra, Southern Technical University, Basrah, Iraq

Abstract

Optical communication system for the next generation of wireless communication systems are an exciting, unparalleled new technology. This paper presents a new visible light positioning algorithm system based on position by utilized neural network which depending on directly measured received signal strength (RSS) information of 3D coordinates. This algorithm is called light positioning algorithm neural network (LPANN) which used 5 laser diodes LDs, each one consists of 5×5 LD chips. In addition, a novel multi Input multiple output (MIMO) orthogonal frequency division multiplexing (OFDM) based VLC systems generalized laser diodes (LD) modulation scheme as second part of this paper that is called Zero Forcing Equalizer Neural network ZFENN algorithm which based on 4 × 4 optical MIMO-VLC. It is accomplished by using LD index modulation and spatial multiplexing. Actual and imaginary parts of the complex time domain OFDM signals are therefore separated first and then, bipolar signals are transmitted through VLC channels by encoding sign-information in LD indexes. In addition, a novel receiver configuration is also suggested for flat frequency or limited channel scenarios. Based on the results of this analysis, the positioning accuracy have been improved, so this is lead to enhance data rate. While, by using the second part of the MIMO-OFDM system that leads to enhancing the SNR and BER more than 10^{-4}which are introduced to eliminate multi-user interference (MUI).

Keywords: Optical Laser Diode, Optical MIMO-VLC, Visible Light Positioning.

Corresponding Author:

Author Name: - Faris Mohammed Ali
Department: - Department, Department of Communications Techniques Engineering, Engineering Technical College,
University: - Al-Furat Al-Awsat Technical University,
Address: - Al-Najaf 31001, Iraq.
E-mail:- fanmnm2018@gmail.com, faris@atu.edu.iq

1. Introduction

Visible light communication (VLC) is a term used to describe WiFi systems that transmit information by modulating the visible light for human eyes [1,2]. Light acts mainly as a light instead of communication source, which may not be the main purpose. The development of visible light emission diodes (LEDs) for light production has become important for the fast-growing study of VLC. If the room is illuminated already with LEDs. It not only reduces the necessary hardware costs, the sharing of resources also saves energy. In recent

year, both industry and academia have developed VLC technology. The main goal of this technology is to make LEDs more common due to their long life, energy consumption, protection of high data and environmental friendliness. In fact, it does not become fresh to use visible light as one of the wireless media [3- 6]. The channel characteristics are dependent on the space size and material characteristics of the reflector surfaces, and at different locations the same mobile VLC station will behave differently. One of the key issues with VLC internal systems is to achieve consistent communication efficiency at different positions without disrupting the critical illumination function. In contrast to various ceiling plans for arranging LED array, the light output is compared [7-11].

A new 12 LED light is proposed to minimize SNR homogeneity, ensuring users achieve nearly equal contact efficiency over one circle, and 4 LED light bulbs in the corner [8]. In square and hollow form, two indoor lights are compared, which demonstrates that the star arrangement inside the room is excellent [11, 12]. Four LED lights at the corner of the room and one LED lights in the central area are mounted to evenly spread the light Modern lighting design. In [11] the lighting characteristics are studied by means of rectangular and circulatory LEDs with a changing distance between lamps and ceiling base. An evolutionary algorithm improvement system for achieving uniform energy distribution and illumination on the communication floor has proposed [12].

Visible light has been a subject of many studies on communications technology. Many methods of positioning have been developed to facilitate visible light contact. This method is based on the use of an optical sensor matrix or a picture sensor combination. This method's poor performance is due to its high construction costs, coupled with slow data transmission during communication. In terms of relatively low cost and the ease of their physical and software specifications, RSS is the best of these approaches. In addition to testing the variables, this approach requires pre-calibration of the position of the ID. A position with only two dimensions can be carried out given the calibration procedures [13, 14, 15].

A new method proposed in [16], which overlaps the period of the U-OFDM and the ACO-OFDM with the same range of DCO-OFDM spectral output. Recently, the VLC literature filed for additional bits transfer with low power consumption has taken MIMO and index modulation communication approaches into considerable consideration. In [30], multi-user status is checked on MIMO-VLC systems. Index modulation procedures that use the communications system building blocks are designed to convey more information, in particular in the efficient use of energy and spectrum in IM / DD applications. Index-based transmission systems offer extra flexibility for phase loss compensation [14]. The most popular type of index modification was proposed for MIMO-VLC systems for Space-Modulation (SM), as proposed in [17].

Akande K. O. et al. [18] studied the low complex detection schemes of the MULT input, multi-output standard transmitter with less amplitude, and phase (MIMO CAP). A substantial improvement in efficiency of the respective linear detection instruments, ZF, and MMSE was defined by ordered successive cancelation of interference (OSIC) (or Zero forcing), and by the minimum mean square mistake detection with optimally ordered successive cancellation of interference (MMSE-OSIC). MMSE-OSIC is also found in Calculates to outperform ZF-OSIC by gaining 1.5 dB, and MMSE-OSIC needs only an improvement from a non-practical maximum likelihood (ML) detector of 5 dB per bit. With respect to contrasting the output complexity of the MIMO CAP system, MMSE-OSIC concluded the best ML detection system.

Upon applying the forward error correction (FEC) on a 1.6 m grid, Rui Bian et al. showed in 2019 that VLC device had a data rate of 15.73 Gb/s. The WaveLength Multiplexing (WDM) device has 4 wavelengths of visible light, centered on double colored mirrors and shapes every wavelength using DCO-OFDM. The data transmission rate of 15,73 Gbit / s is achieved with a BER below the 7 % HDFEC limit, i.e. 3.8x10−3 on wireless communication, 1.6 meters, with adaptive bit loading and optimized device parameters.

In addition, Mohammad Dehghani Soltani et al. addressed the SNR derivation for randomized devices in 2019 using the derived PDF to test the DCO-OFDM's output of the AWGN channel by using randomly directed users (UEs). The typical BER is uniformly rounded and corresponds to the same criteria precisely [19,20].

In this paper, we divided the article into two parts: first part we have presented a new visible light positioning algorithm system based on position, which depending on directly measured received signal strength (RSS) that called light positioning algorithm neural network (LPANN). The second part we have proposed novel 4 optical LD MIMO-VLC-based OFDM system for operation on flat frequencies and narrow frequency channels, this is scheme called Zero Forcing Equalizer Neural network (ZFENN).

2. Methodology of the System Design Model

This work has divided in to two parts: first one we have proposed a new visible light positioning algorithm system based on position by utilized neural network which depending on directly measured received signal strength (RSS) information of 3D coordinates. This algorithm is called light positioning algorithm neural network (LPANN). The second one we propose a new multi-input-multi-output (MIMO) based on optical frequency division multiplexer (OFDM) systems algorithm based on line neural network. This algorithm is called (OFDM-LNN) to operate over frequency of VLC channel.

2.1 Light positioning algorithm neural network (LPANN)

The proposed positioning schematic system is shown in Figure 1. Where, considers the receiver is placed at center of room Rx. As well as, we supposed the system consist of five units of illumination sources LDs, each optical illumination sources unit consists of 5×5 LD chips, thus the total number of LD chips is 125 chips are distributed on the ceiling of the room. The optical receiver Rx is under the scope of the sources. Each source independently operates a different unique sinusoidal frequency signal.

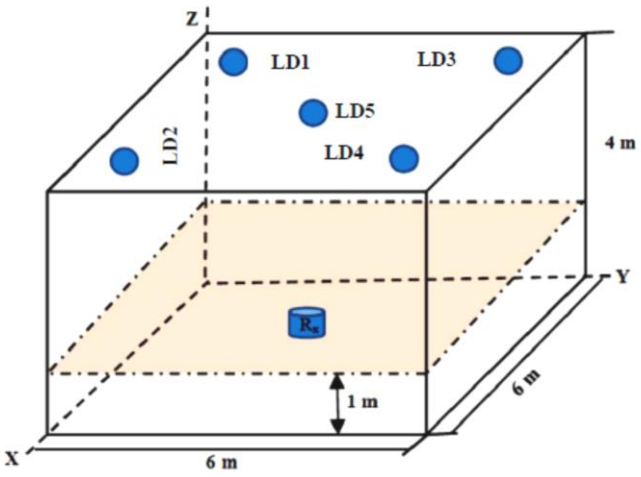

Figure 1. Positioning schematic system

In the proposed system, The RSS is used to infer the distances of the receiver on the ceiling from the LD, and after this triangulation the receiver will be found.

A 3D positioning system X, Y, Z are calculated for the receiver R(x,y), as shown in Figure1 (Note: Z is fixed as Z=1m) based on the RSS values extracted from the five primary sources.

The process of calculation for the internal positioning system is implemented. It is obvious to use a fingerprint based on RSS. Through two consecutive and coordinated processes as shown in Figure 2. The first is the process of system training and the extraction of a database of arithmetically derived values for the RSS.

$$X_{error} = X_{db} - X_{rt} \quad (1)$$

$$Y_{error} = Y_{db} - Y_{rt} \quad (2)$$

Where, Xdb, Ydb are the x-, y- values from the database and Xrt , Yrt are the x-, y- values of real time readings. The second stage is the site extraction technique based on the comparison of the actual RSS values with the RSS values stored in the database prepared.

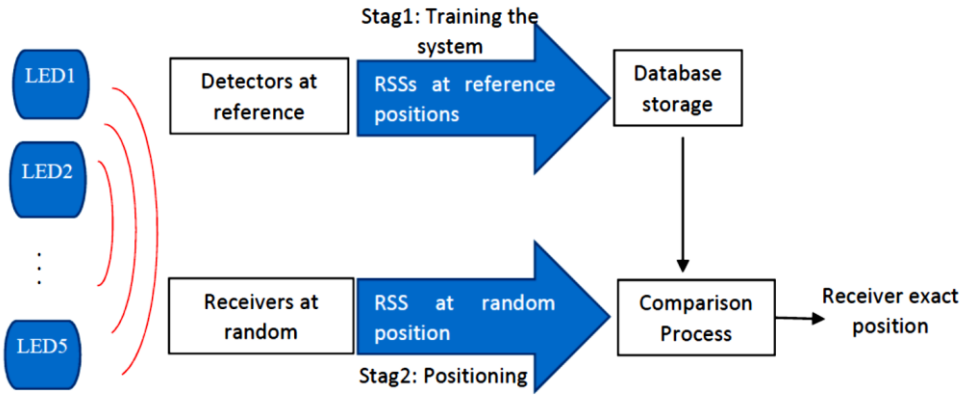

Figure 2. Scheme to calculation RSS

2.2 Principle of optimization

Based on Figure 2, the first step is transmitted power of data communications that will be calculated at different LD sites to achieve a uniform distribution of signal-to-noise ratio (SNR) at the receiver plane. The receiving power in channel modeling, SNR is expressed as one of the most important criteria when discussing system performance will be discussed in this sub-section. In this system, there are N-LD locations distributed uniformly on the room ceiling. A Lambertian radiation pattern is used for each LD. In addition, P receivers are located at 1 m above the ground uniformly on the work plane.

However, the total received power is given by

$$P_r = \sum_{i=1}^{NT} H_i(0) P_i \quad (3)$$

Where, NT is the number of transmitters, Hi(0) and Pi are the directed path channel (DC) gain on the directed path and instantaneous emitted power for the i-th LD chips, respectively.

However, the SNR can be expressed in the photodetector (PD) in a responsible manner, the receiving optical power, and the noise variation as well [21]:

$$SNR = \frac{Pr^{2}}{(\gamma_{shot}+\gamma_{amlifier})2} \quad (4)$$

Where (γ_{shot}) is the shot noise variance can be given as[22]

$$\gamma_{shot} = 2q\ R_r(P_{r_{Total}})B_n + 2q\ I_{sunlight} I_2 B_n \quad (5)$$

In addition, $\gamma_{amplifier}$ is the amplifier noise variance that is given by:

$$\gamma_{amplifier} = {I_{amp}}^{2} * B_a \quad (6)$$

Where q is the Electron charge, Rr is the Photodiode responsively, Bn is the noise bandwidth and $I_{sunlight}$ is the background. current whose traditional. values are 5100 µA given direct exposure to sunlight and 740 µA assuming. indirect. exposure. to sunlight, I2 the noise bandwidth factor which equal to 0.562, I_{amp} is the Amplifier noise density and Ba is the Amplifier bandwidth. [21]

The illumination can be expressed in terms of the photodetector (PD) responsibly as well:

$$L_{amb} = \frac{I}{h\_dis^2} \times \cos\theta \quad (7)$$

Where I the luminous intensity in angle, and it can be calculated by:

$$I = \frac{I_0}{\cos \varphi^m} \quad (8)$$

I0 is the center luminous intensity of an LD. The parameters that used in LPANN algorithm has shown in Table 1.

Table 1. Positioning VLC simulation parameterises

Parameters	Value
φ Transmitter Semi-angle (FOV)	85^0
θ incident angle	120^0
Room dimension (L×W×H)	6×6×3 (m^3)
ARX the photodiode active area	0.5 (mm)
LD array Chips	5×5
P_{LD}	2 (mW)
R_r	0.55 (A/W)
B_a	$4.5e^6$ (Hz)
I_{amp}	$5e^{-12}$ (A/Hz0.5)
I_0	24 cd)

2.3 OFDM diagram using zero forcing equalizer neural network ZFENN Algorithm for MIMO system

To the best of our knowledge, we have used a novel modem scheme of Discrete Fourier Transform-Spread-OFDM Technique (DFT-S-OFDM) as shown in Figure 3. We used *M, N_d, N_f, F_s and N_s* as; M is modulation index order, N_d is the number of subcarriers, N_f is the Points of FFT, *Fs* is the sample rate, and finally N_s is the number of transmitted symbols. Where,

Given i = 0, 1, ….., N_s-1, the $x_1^{(i)} \in C^{Nf}$ has a takes structure

$$\boldsymbol{x_1^{(i)}} = [\boldsymbol{0, D_0^{(i)}, D_1^{(i)}, D_2^{(i)}, \dots, D_{Nd-1}^{(i)}, \left(D_{Nd-1}^{(i)}\right)^*, \dots, D_0^{(i)}]^T} \quad \textbf{(9)}$$

Where $\left[x_1^{(i)}\right]_0$ and $\left[x_1^{(i)}\right]_{\mathrm{Nf}/2}$ are assigned N_f / *2* as zeros to remove the DC component. Therefore, this step leads to $N_d = N_f / 2 - 1$. Then $\boldsymbol{x_2^{(i)}} \in \boldsymbol{R^{Nf}}$ is obtained by

$$[x_2^{(i)}]_m = \frac{1}{\sqrt{Nf}} \sum_{n=0}^{N_f-1} [x_1^{(i)}]_n e^{\left(j\frac{2\pi}{Nf}mn\right)} \quad (10)$$

$$= \frac{2}{\sqrt{N_f}} \sum_{n=0}^{N_f/2-1} R\left\{[x_1^{(i)}]_n e^{\left(j\frac{2\pi}{Nf}mn\right)}\right\} \quad (11)$$

Where $\boldsymbol{R}$ is the pure rate of the system and *m* is the minimum-batch size. At the same time, the original signal is expressed in the training package by $\boldsymbol{X_2} = \left[\boldsymbol{x_2^0, x_2^1, x_2^2, \dots x_2^{(Ns-1)}}\right] \in \boldsymbol{L^{N_f \times Ns}}$ **,** the normalize $\boldsymbol{X_2}$ the interval must be [−1, 1] to alleviate the phasing problem of fading in the training stage.

$$L = M \times \frac{N_d}{N_f} \times F_s \quad \textbf{(12)}$$

Where, in the modulation technique part, no Hermitianl symmetry and DC bias have used to ensure that the baseband signals are in real and imaginary domains to operate through frequency flat optical channels. Thus, signals will be sent through the MIMO-Optical channels using the active light-based modulation index (LD). In addition, there is a novel MAP estimator for the calculation of certain real and imaginary parts of the OFDM signals at the receiver. The OFDM modulator processes a complex frequency-domains OFDM structure x_F directly in the proposed scheme without the need for Hermitian symmetry. In order to solve bipolar (positive and negative) elements values of VLC channel, a new MIMO transmission technology based on LD index

modulation being developed. Upon conversion from parallel to serial (P/S), complex signal x_k is distinguished between the real and imaginary parts in $x_k = x_{K,r} + j\, x_{k,i}$, Then the real result, But the following positive real-value signals are interpreted by non-negative separators (+ /−) [22]:

$$X_{k,r}^{+} = \begin{cases} X_{k,r} & If \quad X_{k,r} > 0 \\ 0 & If \quad X_{k,r} < 0 \end{cases} \tag{13}$$

$$X_{k,r}^{-} = \begin{cases} 0 & If \quad X_{k,r} > 0 \\ -X_{k,r} & If \quad X_{k,r} < 0 \end{cases} \tag{14}$$

$$X_{k,i}^{+} = \begin{cases} X_{k,i} & If \quad X_{k,i} > 0 \\ 0 & If \quad X_{k,i} < 0 \end{cases} \tag{15}$$

$$X_{k,i}^{-} = \begin{cases} 0 & If \quad X_{k,i} > 0 \\ -X_{k,i} & If \quad X_{k,i} < 0 \end{cases} \tag{16}$$

Consequently, signals from the $n_R + n_T$ MIMO-VLC system can be transmitted simultaneously, where n_R and n_T are representative of the numbers of units of the receiver (Rx) and transmitter (Tx). It is to be observed that, for the proposed scheme where it is known in this work as $n_T = 4$, n_T must be divisible by four. The positive OFDM time samples and the real value $X_{k,r}^{+}, X_{k,r}^{-}$, $X_{k,i}^{+}$ and $X_{k,i}^{-}$are sent via the optical MIMO-VLC channel (n_R x 4) for *k=0,1,2,...,N-1* that will be represented by H.

$$y = Hx + n \tag{17}$$

where ***y*** is the vector of received signals, ***n*** is additive white Gaussian noise (AWGN), and the transmitted signal vector $x \in R^{4*1}$ formed as

$$x = \begin{bmatrix} x_{k,r}^{+} & x_{k,r}^{-} & x_{k,i}^{+} & x_{k,i}^{-} \end{bmatrix}^{T} \tag{18}$$

Where the transpose of a matrix/vector is expressed by $(.)^{T}$.

According to equations (13-16), in the case of a certain OFDM signal, there are only two out of four ***x*** elements non-zero, i.e. two LDs (emitting light). However, in this section of article, n_R=4 is considered as simple to send, therefore the 4 × 4 optical MIMO-VLC channel is represented by equation 19:

$$H = \begin{bmatrix} h_{1,1} & h_{1,2} & h_{1,3} & h_{1,4} \\ h_{2,1} & h_{2,2} & h_{2,3} & h_{2,4} \\ h_{3,1} & h_{3,2} & h_{3,3} & h_{3,4} \\ h_{4,1} & h_{4,2} & h_{4,3} & h_{4,4} \end{bmatrix} \tag{19}$$

Where ($h_{no.\,,\,no.}$) represented *as* $h_{r,\,t}$ which indicates the optical wireless channel gain connection from the Tx unit (t) to the Rx unit (r) where (t, r) {1, 2, 3, 4}.

The calculation the relationship between SNR and $BER_{RZ\text{-}OOK}$ has achieved by utilizing following equation [21]:

$$BER_{NRZ-OOK} = \frac{1}{2} erfc\left(\frac{1}{2\sqrt{2}}\sqrt{SNR}\right) \tag{20}$$

The received signal vector ***y*** cannot directly be transmitted to the OFDM demodulator, provided that the first thing to obtain the frequency domain estimate OFDM block x_F is to create complex valued signals. Using a Zero

Forcing Equalizer (ZFE) to provide an approximation of ***x*** simply as is straightforward solution to the estimation problem described in equation 17.

$$\hat{x}^{ZF} = H^{-1}y \quad (21)$$

After this process, by selecting the $\hat{x}^{ZF}$ higher magnitude signals, the receiver will evaluate the active LDs indices and corresponding signals. The ZFE estimator is simple, but does not consider a prior knowledge on the probable distribution of ***x*** and can therefore produce negative estimates. Therefore, in order to correct the above drawbacks of the ZFE estimator, we are providing a new MAP estimator for the OFDM scheme, in consideration of prior information that we have for the signal vector ***x***.

The matrix of channel **H** is defined as **H**= [h_1 h_2 h_3 h_4] and can be rewritten according to the signal in equation (17)

$$y = (x \times h) + n \quad (22)$$

Where, given the impulse *h* as h_m and h_n, $m \in \{1, 2\}$, $n \in \{3, 4\}$, therefore equation 22 become

$$y = (h_m x_{k,r} + h_n x_{k,i}) + n \quad (23)$$

Thus, conditional MAP estimates calculations of $x_{k,r}$ and $x_{k,i}$ are necessary for a given pair (m, n) which written as:

$$\left(\tilde{x}_{k,r}^{(m,n)}, \tilde{x}_{k,i}^{(m,n)} = arg_{x_{k,r},x_{k,i}} \min M^{MAP}(m, n, x_{k,r}, x_{k,i})\right) \quad (24)$$

Where $M^{MAP}(m, n, x_{k,r}, x_{k,i})$ is the metric of MAP estimates defined as

$$M^{MAP}\left(m, n, x_{k,r}, x_{k,i}\right) = \left\|y - h_m x_{k,r} - h_m x_{k,i}\right\|^2 + 2\sigma_\omega^2(x_{k,r}^2 + x_{k,i}^2) \quad (25)$$

Where, σ_ω^2 represents the variance and ($\|a\| = a^T a$), following simple algebra handling, equation (25) simplified as:

$$M^{MAP}\left(m, n, x_{k,r}, x_{k,i}\right) = Ax_{k,r}^2 + Bx_{k,i}^2 + Cx_{k,r} + Dx_{k,i} + Ex_{k,r}x_{k,i} \quad (26)$$

Where,

$$\left.\begin{array}{c} A = h_m^T h_m + 2\sigma_\omega^2 \\ B = h_n^T h_n + 2\sigma_\omega^2 \\ C = -2y^T h_m \\ D = -2y^T h_n \\ E = 2h_m^T h_n \end{array}\right\} \quad (27)$$

The $M^{MAP}\left(m, n, x_{k,r}, x_{k,i}\right)$ derivative with regard to $x_{k,r}$ and $x_{k,i}$ equates to zero and yields, conditional on (m,n), and so is the MAP estimates for $x_{k,r}$ and $x_{k,i}$

$$\tilde{x}_{k,r}^{(m,n)} = \left[\frac{2BC-ED}{E^2-4AB}\right]^+, \tilde{x}_{k,i}^{(m,n)} = \left[\frac{2AD-EC}{E^2-4AB}\right]^+ \quad (28)$$

The conditional MAP estimator calculates $\tilde{x}_{k,r}^{(m,n)}$ and $\tilde{x}_{k,i}^{(m,n)}$ for all possible (m, n) pairs in order to determine the active LD indexes (*i.e. m* and *n* estimates) and the corresponding estimates of $x_{k,r}$ and $x_{k,i}$ and then obtained the unconditional estimates of $\tilde{x}_{k,r}^{(m,n)}$ and $\tilde{x}_{k,i}^{(m,n)}$ as follows:

$$(\hat{m}, \hat{n}) = \arg min_{m,n} M^{MAP}\left(m, n, \tilde{x}_{k,r}^{(m,n)}, \tilde{x}_{k,i}^{(m,n)}\right) \quad (29)$$

Where, $\hat{x}_{k,r}^{MAP} = \tilde{x}_{k,r}^{(\hat{m},\hat{n})}, \hat{x}_{k,i}^{MAP} = \tilde{x}_{k,i}^{(\hat{m},\hat{n})}$

After the calculation of the MAP estimates, the conditional MAP estimator of the GLIM-OFDM scheme decides on the most likely active LD pair *(m , n)* and corresponding estimates of $x_{k,r}$ and $x_{k,i}$ ($\hat{x}_{k,r}^{MAP}, \hat{x}_{k,i}^{MAP}$) by

calculating the MAP estimation metric given by equation 25 for all four scenarios. The combiner calculates the estimation of the OFDM scheme signal complex x_k as:-

$$\hat{x}_{k,r} = \begin{cases} \hat{x}_{k,r}^{MAP}, if\ m = 1 \\ -\hat{x}_{k,r}^{MAP}, if\ m = 2 \end{cases} \quad (30)$$

$$\hat{x}_{k,i} = \begin{cases} \hat{x}_{k,i}^{MAP}, if\ n = 3 \\ -\hat{x}_{k,i}^{MAP}, if\ n = 4 \end{cases} \quad (31)$$

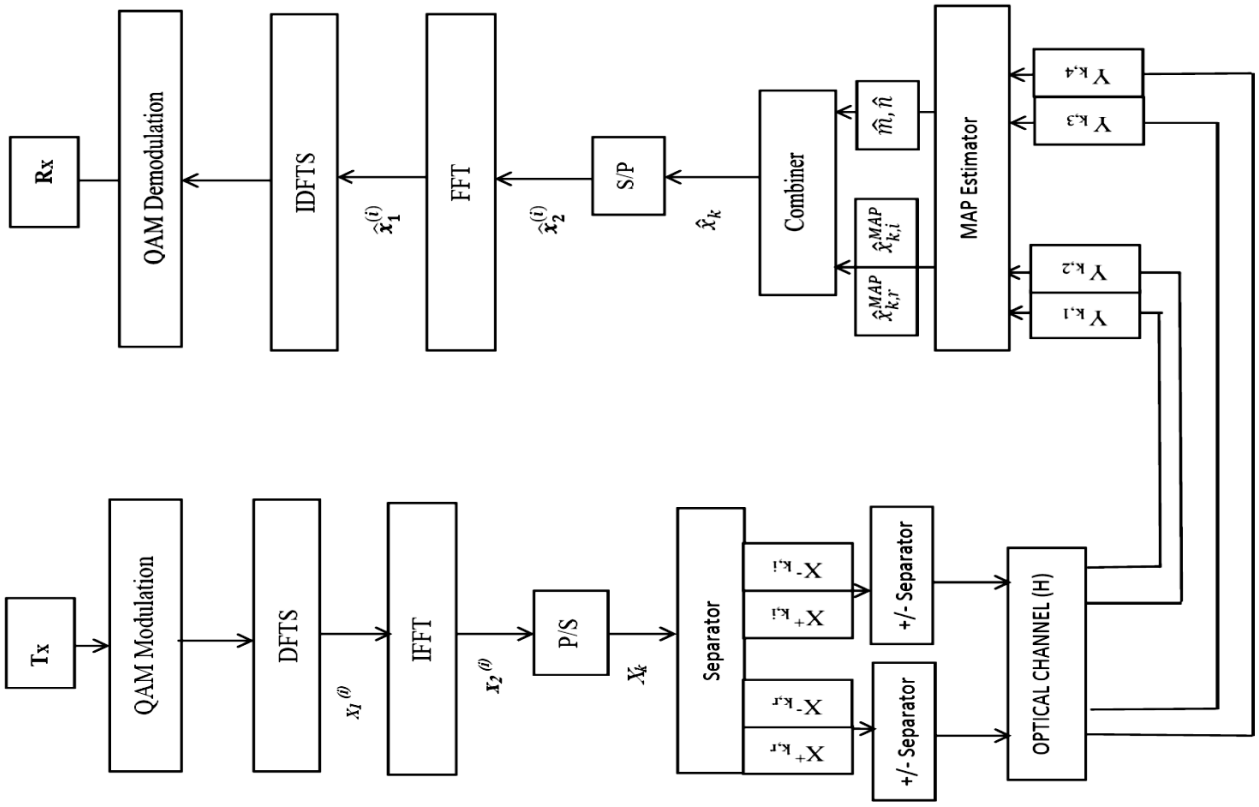

Figure 3. Block diagram of MIMO–OFDM system model

3. Result and discussion

3.1 Positioning using interpolation method

The LDs are located at the room ceiling with coordinates range of LD1(x=-1.5, y=1.5), LD2(x=1.5, y=1.5), LD3 (x=-1.5, y=-1.5), LD4 (x=1.5, y=-1.5), and LD5 (x=0, y=0) which are shown in Figure1. The room is divided into different positions are calculated by using equations 1 and 2 that applying in simulation Matlab. The span between any adjacent Positions is 0.5m.

The plot of the locating error of the proposed interpolation method using RSS has shown in Figure 4. However, the positioning performance using the proposed interpolation method is evaluated, after finishing the construct the database finally, the indoor positioning system utilizing the proposed algorithm for the database is implemented and simulated. As a result, the proposed algorithm can be applied to extend the RSS database, and then the interpolation technique is used to enhance the positioning performance. It is clear that the larger the database, the better the positioning performance. The interpolation method using RSS. The positioning error is too small for an indoor positioning system, at a first sector area (6×6×3 m^3) of the testing room. The RSS values

can be affected by the walls and furniture that did not take into account in this work. A multi-path effect can be caused by these factors, as well as a dispersion in the signal, which means an error in positioning. Suitable parameters selection leads to minimizing the positioning error. As shown in fig (4), a tolerable error caused by the above factors is produced.

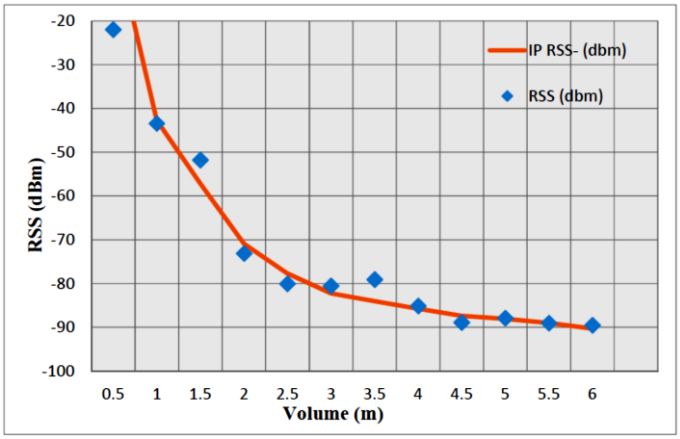

Figure 4. The plot of positioning error of LPANN using RSS

According to our results, the site measurement accuracy is increased from 10 to 15 cm as well as the accuracy of positioning external to the cell.

3.2 Received Power and SNR

The significant contribution to the proposed illumination units configuration model is the fact that it consumes less power in downlink communication as shown in Table 2 where it shows the numerical comparison of the conventional and new configuration model.

Table 2. Coparision between five LD and four LED units model configration

Illumination units in Room	Power per LED and LD	Emitted power signal unit	Total power consumption
4	20mW	72W	288W
5	2 mW	50W	250W

Figure 5 shows the power distribution in the typical room for lighting unit configurations in the proposed model. While, Figure 6 show the Coverage area distribution in the room for the proposed model. In configuring the four typical illumination units, the maximum receiving power is centered in the corners of the room. The center of the room received a little optical power and the SNR distribution and it is interesting that the new LD distribution for the illumination units design produced a new power and SNR distribution in the entire room.

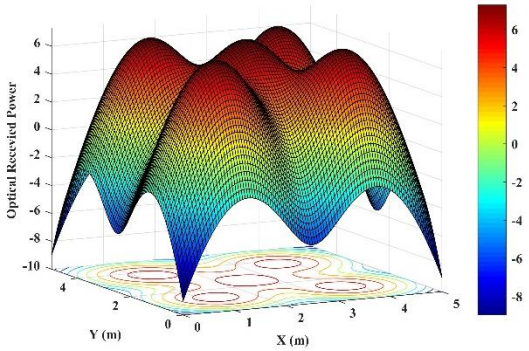

Figure 5. Power distribution in typical room

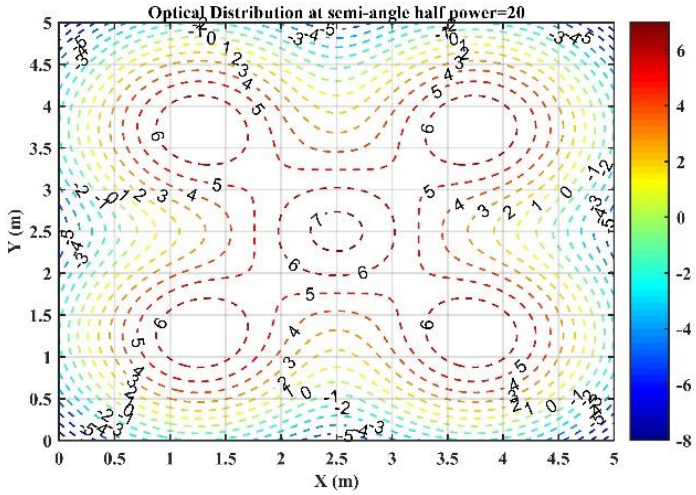

Figure 6. Coverage area distribution in a term of received power

In addition, the SNR signal varies in the range of (47 - 65) at the testing room, as shown in fig (7). Comparing with the reference [23] the SNR can be reached to 42.5 dB at the better case while the SNR in our work reaches to 65 dB at the best point in the room. As well as Fig 8 show the Coverage area distribution in a term of received SNR.

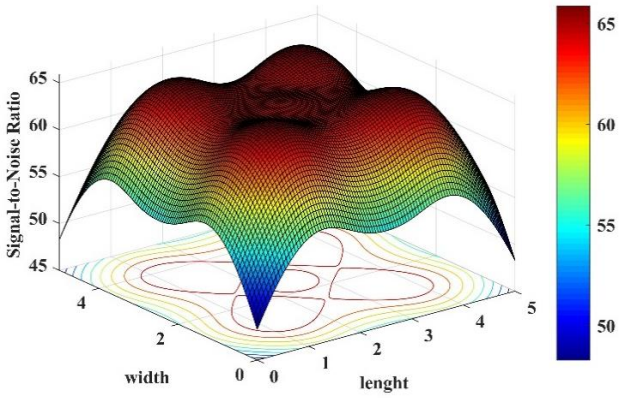

Figure 7. 3D Plot SNR distribution for 5-lds

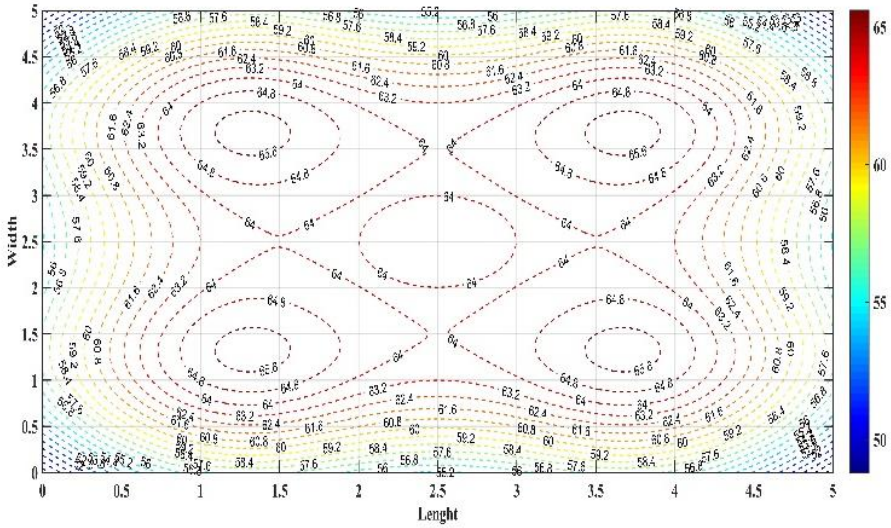

Figure 8. Coverage area distribution in a term of received SNR

According to the results, Figure (9) illustrate the relationship between SNR versus BER by using OFDM scheme with modulation index (M=4). Where it can be notice that the value of SNR is 60 dB with BER is higher than 10^{-4}

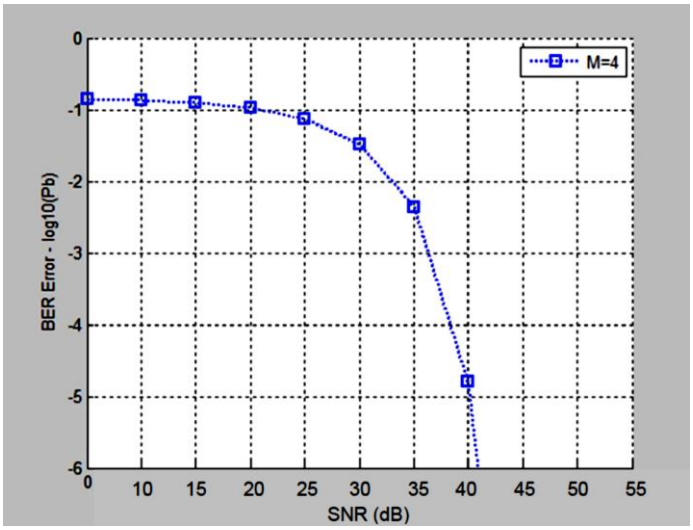

Figure 9. The relationship between SNR and BER for M=4

In order to achieve verifying between our algorithm system results with other algorithm techniques, we make a compression with e-GLIM-OFDM algorithm for modulation index M=4, we found that the SNR is 41 dB with BER is higher than 10^{-4}while SNR was 35 dB with BER is higher than 10^{-2}. Therefore, the SNR obtained in our work is acceptable compared to other work mentioned in [24].

3.3 MIMO-OFDM using NLNNS

Figure (10) illustrate the relationship between SNR Versus BER by using MIMO-OFDM in channel coding with different modulation index (M=4, 8, 16). Where the values of SNR with BER varying with the modulation index. It shows that the SNR are 41, 46 dB with BER is higher than 10^{-4} for M= 4 and 8, respectively. While, for M=16 the SNR is 52 dB with and BER is above 10^{-4} Where the relationship SNR vs. BER are addressed by eq. (24).

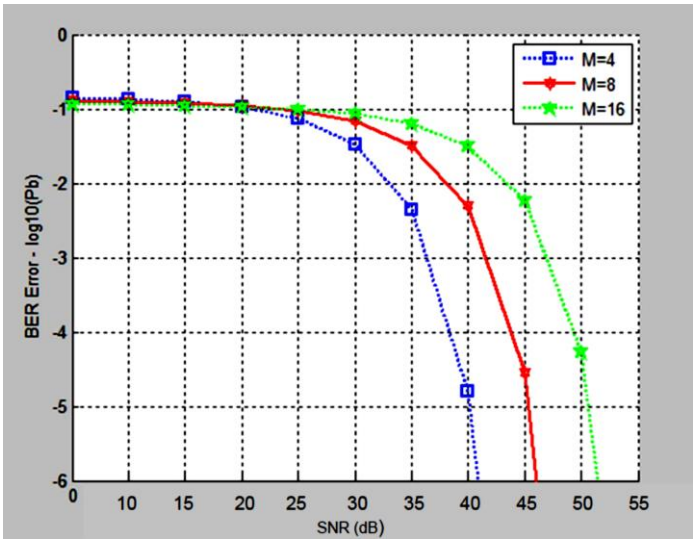

Figure 10. The relationship between SNR and BER for MIMO

4. Conclusion.

This paper is focused on design and evaluation of the positioning and MIMO-OFDM for the optical system (visible light communication) by using laser diodes (LDs), where the simulation was carried out in a room with dimensions of (6×6x3) m^3. A 3D indoor positioning algorithm system has been used to found the RSS by using interpolation method. Where this proposed system offers high gains of accuracy in a positioning system, furthermore, a 3D positioning results with positioning error of less than 15 cm in a coverage volume of is verified enhancement in SNR and data rate. On the other hands, the NLNNS algorithm of DFT-S OFDM, which is used to determine the MIMO-OFDM. So, according to the results of BER, we can show the performance of the system within the channel codding has improvement, where the value was more than 10^{-4}. Compared with the results of the e-GLIM method. As well as, the enhancement of SNR has achieved by the value 60 dB and around 67.5, 75 dB for M=8, 16, respectively.

5. References

[1] S. Arnon, J. Barry, G. Karagiannidis, R. Schober, and M. Uysal," *Advanced optical wireless communication systems*," Cambridge university press, 2012.

[2] Ozlam Abdulhakeem Mahmood, Mohammed Ahmed Hussein, Aras Al-dawoodi, Heyam Maraha, "Random weather phenomena in free-space optical - FTTx communication system, " *Periodicals of Engineering and Natural Sciences*, vol. 8, no. 2, pp.1060-1066, 2020.

[3] Z. Ghassemlooy, W. Popoola, and S. Rajbhandari, "*Optical Wireless Communications: System and Channel Modelling with Matlab*," CRC press, 2012.

[4] Sarab Ahmed Amen, Ali Ismail Salih, Essa Ibrahim Essa, "Software simulation for the study of the fiber optic properties and its impact on the output power, " *Periodicals of Engineering and Natural Sciences* , vol. 8, no. 2, 2020.

[5] C. Medina, M. Zambrano, and K. Navarro," LED Based Visible Light Communication: Technology, Applications and Challenges-A survey," *International Journal of Advances in Engineering & Technology*, 8(4), 2015.

[6] Essa Ibrahim Essa, Ahmad Ayied Ahmad, Mshari A. Asker, Fidan T. Sedeeq, "Transmission power optimization of high speed 32 channels×12.8 Tbps CWDM based on multi-span SSMF using RZ modulation format, " *Periodicals of Engineering and Natural Sciences* , vol. 7, no. 3, 2019.

[7] H. F. Khazaal *et al.*, "A Proposed Model for the Mutual Dependency Between QoE and QoS in Wireless Heterogeneous Networks," vol. 9, no. 2, pp. Page 45-55, 2017.

[8] A. Burton, H. Le Minh, Z. Ghasemlooy, S. Rajbhandari, "A study of LED Lamination Uniformity with Mobility for Visible Light Communications," *International Workshop on Optical Wireless Communications (IWOW) IEEE*, 2012.

[9] I. A. Aljazaery, H. T. S. Alrikabi, and M. R. J. I. J. o. I. M. T. Aziz, "Combination of Hiding and Encryption for Data Security," vol. 14, no. 09, pp. 34-47, 2020.

[10] Z. Wang, C. Yu, W. Zhong, J. Chen, and W. Chen," Performance of a novel LED lamp arrangement to reduce SNR fluctuation for multi-user visible light communication systems. *Optics Express*, 20(4): pp. 4564-4573, 2012.

[11] H. Chun, C. J. Chiang, A. Monkman, and D. O'Brien," A study of illumination and communication using organic light emitting diodes, *Journal of Lightwave Technology*, 31(22), pp 3511-3517, 2013.

[12]

H. Alrikabi, A. H. Alaidi, and K. J. I. J. o. I. M. T. Nasser, "The Application of Wireless Communication in IOT for Saving Electrical Energy," vol. 14, no. 01, pp. 152-160, 2020.

[13] L. Al-Hakim Azizan, M. S. Ab-Rahman, and K. Jumiran," Analytical approach on SNR performance of visible light communication for modern lighting layout, *International Conference on Innovation Management and Technology Research, IEEE*, 2012.

[14] C. W. Chow, Y. Liu, C. H. Yeh, J. Y. Sung, and Y. L. Liu," A practical in-home illumination consideration to reduce data rate fluctuation in visible light communication, *IEEE Wireless Communications*, 22(2), pp. 17-23, 2015.

[15] J. Ding, Z. Huang, and Y. Ji," Evolutionary algorithm based uniform received power and illumination rendering for indoor visible light communication, *Journal of the Optical Society of America A*, 29(6), pp. 971-979, 2012.

[16] Y. He, L. Ding, Y. Gong, and Y. Wang, "Real-time audio & video transmission system based on visible light communication," *Optics and Photonics Journal*, 3(2), pp. 153-160, 2013.

[17] T. Yamazato, I. Takai, H. Okada, T. Fujii, T. Yendo, S. Arai, M. Andoh, T. Harada, K. Yasutomi, K. Kagawa, "Image-sensor-based visible light communication for automotive applications," *I EEE Communications Magazine*, 52(7), pp. 88-97, 2014.

[18] J. Luo, L. Fan, and H. Li, "Indoor Positioning Systems Based on Visible Light Communication: State of the Art," *IEEE Communications Surveys & Tutorials*, 19(4), pp. 2871-2893, 2017.

[19] H.Lee, I. Lee, and S.H. Lee,"Deep learning based transceiver design for multi-colored VLC systems, *Optics Express*, 26(5), pp. 6222-6238, 2018.

[20] I. Al Barazanchi, H. R. Abdulshaheed, and A. Shibghatullah, "The Communication Technologies in WBAN," *Int. J. Adv. Sci. Technol.*, vol. 28, no. 8, pp. 543–549, 2019.

[21] D. Tsonev and H. Haas, "Avoiding spectral efficiency loss in unipolar OFDM for optical wireless communication, *IEEE International Conference on Communications (ICC)*, 2014.

[22] Q. Wang, Z. Wang, and L. Dai," Multiuser MIMO-OFDM for visible light communications, IEEE Photonics Journal, 7(6), pp. 1-11, 2015.

[23] H. T. Alrikabi, A. H. M. Alaidi, A. S. Abdalrada, and F. T. J. I. J. o. E. T. i. L. Abed, "Analysis the Efficient Energy Prediction for 5G Wireless Communication Technologies," vol. 14, no. 08, pp. 23-37, 2019.

[24] K. O. Akande, F. B. Offiong, H. Alrakah, and W. O. Popoola," Performance Comparison of MIMO CAP Receivers in Visible Light Communication, *11th International Symposium on Communication Systems, Networks & Digital Signal Processing (CSNDSP), IEEE*, 2018.

[25] I. Al Barazanchi, H. R. Abdulshaheed, M. Safiah, and B. Sidek, "Innovative technologies of wireless sensor network : The applications of WBAN system and environment," *Sustain. Eng. Innov.*, vol. 1, no. 2, pp. 98–105, 2020.

[26] Faris Mohammed Ali, Ahmed Ghanim Wadday, Haidar Zaeer Dhaam, Evaluation of performance information downloading of (optical – radio frequency) hybrid system network, " *Periodicals of Engineering and Natural Sciences* , vol. 8, no. 2, 2020.

[27] M. D. Soltani and I. Tavakkolnia," Impact of device orientation on error performance of Li-Fi systems, *IEEE Access*, Vol.7, pp. 41690-41701, 2019.

[28] H. T. S. J. W. J. o. E. S. ALRikabi, "Study the Matching of the Level of Electromagnetic Radiation Emitted by Communication Towers in the Kut City with the International Health organization criterion," vol. 4, no. 1, pp. 101-111, 2016.

[29] Z. Huanhuan," Design and Analysis of Visible Light Communication and Positioning System, Ph.D. *Thesis, National University of Singapore*, 2017.

[30] T. T. Son, H. Le-Minh, F. Mousa, Z. Ghassemlooy, and N. Van Tuan," Adaptive correction model for indoor MIMO VLC using positioning technique with node knowledge," *International Conference on Communications, Management and Telecommunications*, 2015.

[31] H. T. S. Al-Rikabi, *Enhancement of the MIMO-OFDM Technologies*. California State University, Fullerton, 2013.

[32] A. Yesilkaya, F. Miramirkhani, and M. Uysal," Optical MIMO-OFDM with generalized LED index modulation, *IEEE Transactions on Communications*, 65(8), pp. 3429-3441, 2017.